



Resonant scattering of a single atom with gain: A wave-function-diagrammatic approachM. Donaire ^{*}*Departamento de Física Teórica, Atómica y Óptica and IMUVA, Universidad de Valladolid, Paseo Belén 7, 47011 Valladolid, Spain* (Received 1 July 2021; accepted 27 September 2021; published 15 October 2021)

We characterize the optical response of a three-level atom subjected to an incoherent pump and continuously illuminated with a weak quasiresonant probe field. To this end, we apply a wave-function approach based on QED Hamiltonian perturbation theory which allows for a reduction of the atomic dynamics to that of an effective two-level atom and for an implementation of the incoherent effects that respects unitarity. Using a diagrammatic representation, we identify and classify all the radiative processes. This allows us to compute the scattered power, the spontaneous emission, and the stimulated emission, as well as the total cross sections of extinction, absorption, and scattering. We find that, besides a general enhancement of the linewidth and an attenuation of the spectral amplitudes, the pump reduces the nonradiative losses and provides gains in the form of stimulated emission and incoherent radiation. For sufficiently strong pump, gains and losses compensate, resulting in the vanishing of extinction. In particular, for negligible nonradiative losses, extinction vanishes for a pumping rate of $(1 + \sqrt{5})/2$ times that of the natural decay.

DOI: [10.1103/PhysRevA.104.043704](https://doi.org/10.1103/PhysRevA.104.043704)**I. INTRODUCTION AND MOTIVATION**

The scattering of light by a free atomic dipole in its ground state is a subject extensively studied within the standard QED theory, in any regime of physical interest [1–3]. In order to describe the scattering properties of a multilevel atom semiclassically, it is also possible to characterize its optical response to a weak field with an effective linear polarizability [4–9] $\alpha(\omega)$ within the framework of the linear response theory and the T -matrix formalism. Operating this way, radiative dissipation appears parametrized by a term proportional to the imaginary part of the electromagnetic (EM)-field propagator $\text{Im}\{\mathbb{G}\}$, whereas its real part $\text{Re}\{\mathbb{G}\}$ is related to a shift in the atomic transition frequency analogous to that of the Lamb shift [4,7,8,10,11]. In addition, nonradiative losses are accounted for in an effective manner by adding an imaginary damping parameter on top of that proportional to $\text{Im}\{\mathbb{G}\}$ in such a way that the resultant polarizability is compatible with the optical theorem. When illuminated by an external field of frequency ω , $\mathbf{E}_0(\omega)$, the nature of the radiation scattered by the atom is interpreted on the basis of its classical response to the external field. Thus, it is customary to refer to the scattered power in phase with the expectation value of the atomic dipole moment, $\langle \mathbf{d}(\omega) \rangle = \alpha(\omega) \cdot \mathbf{E}_0(\omega)$, as coherent scattered power, $\mathcal{W}_{\text{coh}} \sim \text{Im}\{\omega \langle \mathbf{d}(\omega) \rangle \cdot \mathbf{E}^*(\omega)\}$, with $\mathbf{E}(\omega)$ the field radiated by the dipole itself [12]. Further, in regard to ensembles of atomic dipoles, their internal energy as well as their collective optical response to a weak field are derived out of the single-atom polarizabilities applying multiple scattering techniques within the framework of the linear response theory [4,8,10,13–18]. Finally, when the atoms are coherently driven by stronger external fields, beyond the linear response theory, a nonlin-

ear polarizability for single atoms [19–21] and a nonlinear susceptibility for atomic ensembles [22,23] can be computed within the density-matrix formalism.

Let us consider next an optical medium subjected to an incoherent pump. In order to incorporate the action of the pump in the response of the medium to a weak probe field, inspired by the manner that nonradiative losses are implemented in the aforementioned linear polarizability of an atom, it is tempting to implement the gains by adding an imaginary damping term to its semiclassical dielectric response, of opposite sign with respect to that of the losses. While this procedure is followed in some semiclassical systems (cf. Refs. [24,25]), it does not apply to the case of an atomic medium, e.g., the active medium of a laser subjected to an incoherent pump.¹ On the contrary, as with the aforementioned losses, the period of coherent evolution decreases with the incoherent gains for an atomic system. This is confirmed by the computation of the effective Bloch equations of a three-level atom subjected to an incoherent pump, which can be reduced to those of an effective two-level system integrating out the dynamics of the unstable upper state [27,28]. Further, when the atom is illuminated with a weak probe field $\mathbf{E}_0(\omega)$, an effective polarizability α can be derived from the quantum computation of the induced dipole moment $\langle \mathbf{d}(\omega) \rangle = \alpha(\omega) \cdot \mathbf{E}_0(\omega)$ [12,28]. Next, the computation of the scattered power lies in the application of the aforementioned classical expression for \mathcal{W}_{coh} [12] or in the application of the quantum regression

¹The reason is that, while semiclassical media support bosonlike excitations, the atomic excitations behave as fermions in the sense that the population rates of the atomic states lie within the interval $[0, 1]$. In turn this implies that the period of coherent evolution increases with the gain for a bosonlike system, while it decreases for an atomic system [26].

*manuel.donaire@uva.es

theorem upon the dipole moment quadratic fluctuations [21,29–31]. In either case only the dynamics of the atomic states is treated quantum mechanically, while the scattered power is a derivative product in which the actual nature of the radiation is generally unclear.² As a result, odd results like the vanishing of the scattering cross section are obtained [28].

The aim of this article is to develop a wave-function-diagrammatic approach to study the optical response of a three-level atom to a quasis resonant probe field while subjected to incoherent pumping. To this end we apply time-dependent Hamiltonian perturbation theory, treating the atomic and photonic degrees of freedom on the same footing. This allows us to track the dynamics of both atomic states and photons, to identify and classify all the radiative processes, and to compute cross sections and radiative power without appealing to semiclassical expressions like that for \mathcal{W}_{coh} . We find that, besides a general attenuation of the spectral amplitudes, the pump reduces the nonradiative losses and provides gains in the form of stimulated emission and incoherent radiation. In turn, for a sufficiently strong pump, gains and losses compensate, resulting in the vanishing of extinction, one of the necessary conditions for parity-time-reversal (\mathcal{PT}) symmetry in an optical system [25,33].

The latter finding is intended to pave the way for the extension of the present work to many-atom systems with gains and losses [20,34]. In particular, we will ultimately be interested in engineering the exceptional properties already displayed by some semiclassical optical systems [35]. In a subsequent work we plan to address the optical response of a pair of identical atoms, with one of them continuously pumped, and the study of the anomalies already found in analogous systems related to \mathcal{PT} symmetry [24,25,36].

The article is organized as follows. In Sec. II we describe the fundamentals of the approach. In Sec. III we identify diagrammatically all the radiative processes and compute the corresponding cross sections and emitted power. In Sec. IV we discuss the energetic balance and represent graphically the cross sections in terms of the pump rate. In Sec. V we verify that our results are compatible with unitarity. In passing, we compare our results with those of a semiclassical calculation. The conclusions are summarized in Sec. VI.

II. FUNDAMENTALS OF THE APPROACH

Let us consider a three-level atom, with g , e , and u the ground state, the excited state, and the upper auxiliary state, respectively, with energy intervals $\hbar\omega_0$ between g and e , and $\hbar\omega_u$ between e and u , and natural linewidths γ_0 and γ_u , respectively (see Fig. 1). The atom is continuously illuminated by two linearly polarized monochromatic fields referred to as pump and probe fields, of amplitudes, frequencies, momenta, and polarization vectors E_0 , ω , \mathbf{k} , $\boldsymbol{\epsilon}$ and E_p , ω_p , \mathbf{k}_p , $\boldsymbol{\epsilon}_p$, respec-

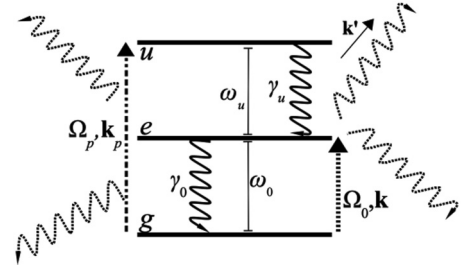


FIG. 1. Schematics of the system under study, consisting of a three-level atom and two external fields. A pump field of strength Ω_p causes the transient excitation of the atom from the ground state g to the upper level u , from which it decays, rapidly and incoherently, to the intermediate level e at a rate γ_u , causing an effective pump rate $\mathcal{P} = \Omega_p^2/\gamma_u$. Energy intervals and dissipative channels are depicted. The atom is illuminated by a weak probe field of strength Ω_0 and momentum \mathbf{k} , quasis resonant with the $g \rightarrow e$ transition. Radiation of momentum \mathbf{k}' is scattered.

tively. For the sake of simplicity, we consider the probe field quasis resonant with the $g \rightarrow e$ transition, $|\omega - \omega_0| \ll \gamma_0$, and the pump field resonant with the $g \rightarrow u$ transition, $\omega_p \approx \omega_0 + \omega_u$. Their corresponding Rabi frequencies are $\Omega_0 = E_0 \boldsymbol{\mu} \cdot \boldsymbol{\epsilon}$ and $\Omega_p = E_p \tilde{\boldsymbol{\mu}} \cdot \boldsymbol{\epsilon}_p$, where $\boldsymbol{\mu} = \langle g|\mathbf{d}|e\rangle$ and $\tilde{\boldsymbol{\mu}} = \langle g|\mathbf{d}|u\rangle$ are the dipole transition moments, with \mathbf{d} the electric dipole operator. Incoherent pumping is achieved with $\gamma_u \gg \Omega_p, \gamma_0$, in which case the fast dynamics of the auxiliary state can be integrated out in an effective manner. Further, the probe field interacts weakly with the effective two-level atom for $\Omega_0 \ll \gamma_0$. In the following we describe our Hamiltonian approach, we quantify the incoherent processes that lead to the reduction of the three-level dynamics to that of an effective two-level atom, and we explain how to account for the quantum interaction of the probe field with the resultant two-level atom.

A. Hamiltonian approach

Our wave-function-diagrammatic approach is based on the time propagator of the atom-EM-field system $\mathbb{U}(t)$. In terms of the Hamiltonian of the system H , it reads

$$\mathbb{U}(t - t_0) = \mathcal{T}\text{-exp}\left(-i\hbar^{-1} \int_{t_0}^t d\tau H(\tau)\right), \quad (1)$$

where $\mathcal{T}\text{-exp}$ stands for time-ordered exponential. H contains a free component H_0 and an interaction term W . As for the free Hamiltonian it reads

$$H_0 = \hbar\omega_0 |e\rangle \langle e| + \hbar(\omega_0 + \omega_u) |u\rangle \langle u| + \sum_{\mathbf{k}', \boldsymbol{\epsilon}'} \hbar\omega' \left(a_{\mathbf{k}', \boldsymbol{\epsilon}'}^\dagger a_{\mathbf{k}', \boldsymbol{\epsilon}'} + \frac{1}{2} \right),$$

where the second term corresponds to the free EM Hamiltonian, with $a_{\mathbf{k}', \boldsymbol{\epsilon}'}^\dagger$ and $a_{\mathbf{k}', \boldsymbol{\epsilon}'}$ the creation and annihilation operators, respectively, of photons of momentum \mathbf{k}' , frequency $\omega' = ck'$, and polarization vector $\boldsymbol{\epsilon}'$. The atom-field interaction is, in the electric dipole approximation,

$$W = -\mathbf{d} \cdot \mathbf{E}(\mathbf{r}_A),$$

²In some particular scenarios, however, within the density-functional formalism, the photonic dynamics is also addressed. That is the case of, for instance, the dressed-atom formalism for an atom interacting with a strong probe field [32] or the Jaynes-Cummings model in cavity QED, where the spectrum of cavity modes is a subject of study [26].

where \mathbf{r}_A is the atomic center of mass. In Schrödinger's picture, the electric-field operator can be expanded as a sum over normal modes

$$\begin{aligned} \mathbf{E}(\mathbf{r}) &= i \sum_{\mathbf{k}', \epsilon'} \sqrt{\frac{\hbar \omega'}{2\epsilon_0 \mathcal{V}}} [\epsilon' a_{\mathbf{k}', \epsilon'} e^{i\mathbf{k}' \cdot \mathbf{r}} - \epsilon'^* a_{\mathbf{k}', \epsilon'}^\dagger e^{-i\mathbf{k}' \cdot \mathbf{r}}] \\ &= \sum_{\mathbf{k}', \epsilon'} [\mathbf{E}_{\mathbf{k}', \epsilon'}^{(+)}(\mathbf{r}) + \mathbf{E}_{\mathbf{k}', \epsilon'}^{(-)}(\mathbf{r})]. \end{aligned} \quad (2)$$

Essential in our calculations is the vacuum expectation value of the quadratic fluctuations of the electric field, which reads

$$\begin{aligned} \sum_{\epsilon'} \int_0^{4\pi} \frac{d\Theta_{\mathbf{k}'}}{8\pi^2} \langle 0 | \mathbf{E}_{\mathbf{k}', \epsilon'}^{(+)}(\mathbf{r}) \mathbf{E}_{\mathbf{k}', \epsilon'}^{(-)}(\mathbf{r}') | 0 \rangle \\ = \frac{-\hbar c}{\epsilon_0} \text{Im} \mathbb{G}(\mathbf{r} - \mathbf{r}'; \omega'). \end{aligned}$$

Here $\mathbb{G}(\mathbf{r} - \mathbf{r}'; \omega')$ is the dyadic Green's function of the electric field induced at \mathbf{r} by an electric dipole of frequency ω' located at \mathbf{r}' ,

$$\mathbb{G}(\mathbf{R}; \omega') = -\frac{k' e^{ik'R}}{4\pi} \left[\frac{\mathbb{P}}{k'R} + \frac{i\mathbb{Q}}{(k'R)^2} - \frac{\mathbb{Q}}{(k'R)^3} \right], \quad (3)$$

where the tensors \mathbb{P} and \mathbb{Q} read $\mathbb{P} = \mathbb{I} - \mathbf{R}\mathbf{R}/R^2$ and $\mathbb{Q} = \mathbb{I} - 3\mathbf{R}\mathbf{R}/R^2$, with $\mathbf{R} = \mathbf{r} - \mathbf{r}'$, and $k' = \omega'/c$. Considering W as a perturbation to H_0 , the time propagator of the system admits an expansion in powers of W which can be developed from its time-ordered exponential expression

$$\begin{aligned} \mathbb{U}(t - t_0) \\ = \mathbb{U}_0(t) \mathcal{T}\text{-exp} \left(\int_{t_0}^t -i\hbar^{-1} d\tau \mathbb{U}_0^\dagger(\tau) W \mathbb{U}_0(\tau - t_0) \right), \end{aligned} \quad (4)$$

where $\mathbb{U}_0(t - t')$ is the unperturbed time propagator $\mathbb{U}_0(t - t') = \exp[-iH_0(t - t')]$.

B. Incoherent dynamics with the pump field: Effective two-level atom

Let us consider first the action of the pump field alone under the condition $\gamma_u \gg \Omega_p, \gamma_0$. The corresponding quantum state of the EM field is defined by

$$|N_{\mathbf{k}_p, \epsilon_p}\rangle = \frac{1}{\sqrt{N_{\mathbf{k}_p, \epsilon_p}!}} (a_{\mathbf{k}_p, \epsilon_p}^\dagger)^{N_{\mathbf{k}_p, \epsilon_p}} |0\rangle,$$

where $N_{\mathbf{k}_p, \epsilon_p}/\mathcal{V} = \epsilon_0 E_p^2/\hbar\omega_p$ is the pump-photon density, with \mathcal{V} a quantization volume, and $|0\rangle$ is the EM vacuum state. The incoherent dynamics is determined by the rapid decay of the atom from the state u to e after the action of the pump upon the atom in state g [Fig. 2(a)], and by the slow decay from the state e to g [Fig. 2(b)]. Considering these phenomena as Markovian, they are the result of a series of consecutive processes of emission and reabsorption of single photons. The addition of all the diagrams in Fig. 2(a) yields, for the rate of

the incoherent pump transition $\mathcal{P} = d|\langle e | \mathbb{U}(t) | g \rangle|^2/dt$,

$$\begin{aligned} \mathcal{P} &= -2 \frac{\Omega_p^2}{\gamma_u^2} \frac{(\omega_u - \omega_0)^2}{\hbar\epsilon_0 c^2} \hat{\boldsymbol{\mu}} \cdot \text{Im} \mathbb{G}(\mathbf{R}; \omega_u - \omega_0) \cdot \hat{\boldsymbol{\mu}} \\ &= \frac{\Omega_p^2}{\gamma_u}, \quad R \rightarrow 0^+, \end{aligned} \quad (5)$$

where $\hat{\boldsymbol{\mu}} = \langle u | \mathbf{d} | e \rangle$ and in the last equality we identify

$$\gamma_u = -\frac{2(\omega_u - \omega_0)^2}{\hbar\epsilon_0 c^2} \hat{\boldsymbol{\mu}} \cdot \text{Im} \mathbb{G}(\mathbf{R}; \omega_u - \omega_0) \cdot \hat{\boldsymbol{\mu}}, \quad R \rightarrow 0^+.$$

The reading of Fig. 2(a) in terms of quantum states and operators is compiled in Appendix A 1. For the sake of completeness, the rate of spontaneous decay from e to g from the diagrams in Fig. 2(b) is

$$\gamma_0 = \frac{-2\omega_0^2}{\hbar\epsilon_0 c^2} \boldsymbol{\mu} \cdot \text{Im} \mathbb{G}(\mathbf{R}; \omega_0) \cdot \boldsymbol{\mu}, \quad R \rightarrow 0^+. \quad (6)$$

For $\gamma_u \gg \Omega_p, \gamma_0$, the dynamics of the state u can be integrated out adiabatically. In terms of the usual nomenclature of the density functional formalism, this implies the approximation $\mathcal{P}\rho_{gg} \approx \gamma_u \rho_{uu}$, which leads to the following Bloch equations for the effective two-level atom:

$$\partial_t \rho_{ee} = -\gamma \rho_{ee} + \mathcal{P} \rho_{gg}, \quad (7)$$

$$\partial_t \rho_{gg} = \gamma \rho_{ee} - \mathcal{P} \rho_{gg}, \quad (8)$$

$$\partial_t \rho_{eg} = \frac{-(\gamma + \mathcal{P})\rho_{eg}}{2} - i\omega_0 \rho_{eg}. \quad (9)$$

In these equations we have allowed for nonradiative contributions to the decay rate from e to g , γ_{nr} , by introducing

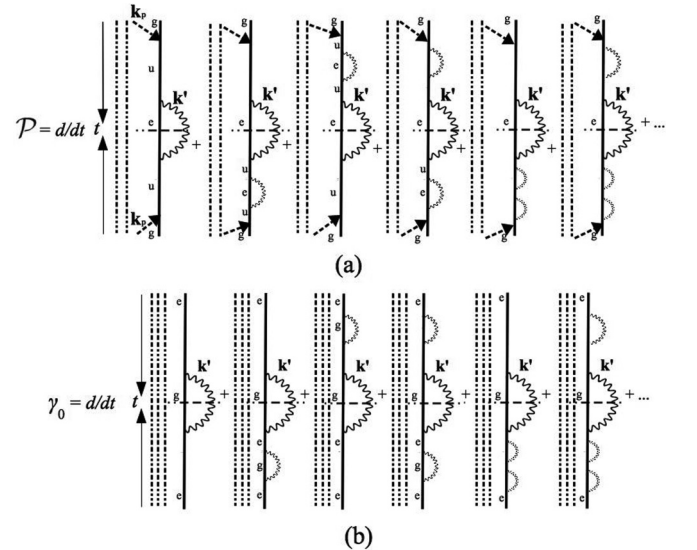


FIG. 2. Diagrammatic representation of the processes that contribute to the pump rate \mathcal{P} and to the spontaneous decay rate γ_0 . Time runs along the vertical axis towards the observation time t . Interacting photons of the pump field with momentum \mathbf{k}_p are depicted with straight dash-dotted arrows. In the weak-coupling regime $\Omega_p \ll \gamma_u$, we restrict ourselves to one-photon interactions. Vertical dash-dotted lines stand for noninteracting-spectator photons, while emitted photons of undefined momentum \mathbf{k}' appear as wavy lines.

$\gamma = \gamma_{nr} + \gamma_0$ in the place of γ_0 . Let us note that these equations take account of the effective dynamics of the atomic degrees of freedom only, which are the ones of interest in the incoherent dynamics. Equivalent equations are obtained starting with Bloch's equations for the three states [26–28]. When dealing with the photonic degrees of freedom in our wave-function formalism, these equations will provide the attenuating factors associated with the incoherent processes. From Eq. (9) for the coherence element ρ_{eg} we read that the pump attenuates the coherent evolution between the two levels [26]. Defining $\Gamma = \gamma + \mathcal{P}$, straightforward integration of the above equations leads to the solutions

$$\rho_{ee}(t) = \frac{\mathcal{P}}{\Gamma}(1 - e^{-\Gamma t}) + N_e e^{-\Gamma t}, \quad (10)$$

$$\rho_{gg}(t) = \frac{\gamma}{\Gamma}(1 - e^{-\Gamma t}) + e^{-\Gamma t}(1 - N_e), \quad (11)$$

$$\rho_{eg}(t) = \sqrt{N_e - N_e^2} e^{-i\omega_0 t} e^{-\Gamma t/2}, \quad (12)$$

where N_e is the population of the excited state at $t = 0$. For asymptotic times $\Gamma t \gg 1$, the atomic populations converge to the steady values $\rho_{gg}(t \rightarrow \infty) = \gamma/\Gamma$ and $\rho_{ee}(t \rightarrow \infty) = \mathcal{P}/\Gamma$, while the coherence element vanishes at a rate Γ regardless of the initial conditions.

C. Wave-function approach with the probe field

Having parametrized the effective action of the pump field with the pump rate \mathcal{P} , we omit its contribution to the quantum EM state hereafter and consider the contribution of the probe-field photons only,

$$|N_{\mathbf{k},\epsilon}\rangle = \frac{1}{\sqrt{N_{\mathbf{k},\epsilon}!}} (a_{\mathbf{k},\epsilon}^\dagger)^{N_{\mathbf{k},\epsilon}} |0\rangle,$$

where $N_{\mathbf{k},\epsilon}/\mathcal{V} = \epsilon_0 E_0^2 / \hbar \omega$ is the photon density and $\epsilon_0 c E_0^2 / 2$ is the time-averaged intensity. Therefore, once the atomic state has reached its steady state, the atom-EM-field state is a mixed state made of the incoherent superposition of the pure states

$$|\Psi_0\rangle_g = \sqrt{\gamma/\Gamma} |N_{\mathbf{k},\epsilon}; g\rangle, \quad |\Psi_0\rangle_e = \sqrt{\mathcal{P}/\Gamma} |N_{\mathbf{k},\epsilon}; e\rangle, \quad (13)$$

where we have included the statistical weights $\sqrt{\gamma/\Gamma}$ and $\sqrt{\mathcal{P}/\Gamma}$, respectively. It is upon the statistical mixture of these states that quantum perturbation theory is to be applied in the computation of the optical response. Thus, the physical quantities to be calculated are statistical averages over the quantum expectation values computed upon the pure states $|\Psi_0\rangle_g$ and $|\Psi_0\rangle_e$.

For a weak probe field $\Omega_0 \ll \Gamma$, the optical response of the atom at leading order involves terms of up to $O(W^4)$ in \mathbb{U} in Eq. (4). They are represented diagrammatically in Fig. 3. In all of them, except for diagram (5), two of the interaction vertices W create or annihilate one photon of the probe field each.

Finally, from Eq. (9) we read that the coherent transitions from steady to intermediate states, say, from $|\Psi_0\rangle_g$ to $|N_{\mathbf{k},\epsilon}, 1_{\mathbf{k}',\epsilon'}; e\rangle$ or from $|\Psi_0\rangle_e$ to $|N_{\mathbf{k},\epsilon}, 1_{\mathbf{k}',\epsilon'}; g\rangle$ in a time interval t , get attenuated in time at an effective rate $\Gamma/2$. That is, at leading order in W , using Eq. (4), $\langle N_{\mathbf{k},\epsilon}, 1_{\mathbf{k}',\epsilon'}; e | \mathbb{U}(t) | \Psi_0\rangle_g \sim \sqrt{\gamma/\Gamma} \int_0^t d\tau e^{-\Gamma(t-\tau)/2} e^{-i(\omega_0+\omega)(t-\tau)} \langle e | \mathbf{d} | g \rangle$.

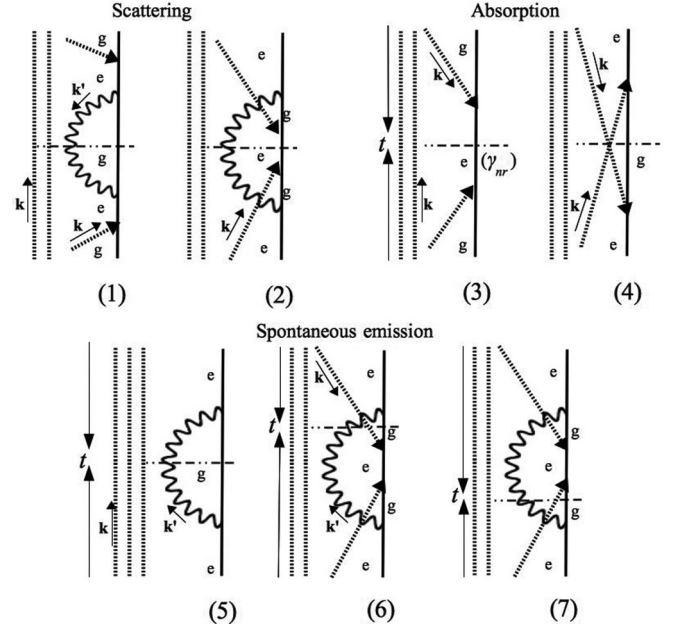


FIG. 3. Diagrammatic representation of the seven processes that contribute, at leading order, to the single-atom cross sections of scattering [(1) and (2)] and absorption [(3) and (4)], as well as to spontaneous emission (5)–(7). The symbol (γ_{nr}) in diagram (3) indicates that only nonradiative dissipation is to be accounted for in that process. Time runs along the vertical axis towards the observation time t . Interacting photons of the incident probe field with momentum \mathbf{k} are depicted with straight dashed arrows. In the weak-coupling regime $\Omega_0 \ll \Gamma$, we restrict ourselves to one-photon interactions. Vertical dashed lines stand for noninteracting-spectator photons, while emitted photons of undefined momentum \mathbf{k}' appear as wavy lines. The incoherent superposition of the states $|\Psi_0\rangle_g$ and $|\Psi_0\rangle_e$ implies the absence of interference between the wave functions of both states.

III. IDENTIFICATION OF RADIATIVE PROCESSES: COMPUTATION OF POWER AND CROSS SECTIONS

Let us consider the atom in the steady state of Eq. (13), continuously illuminated by the weak and quasiresonant probe field of strength Ω_0 and frequency ω as outlined in Sec. II. In the following we identify all the radiative and nonradiative processes which contribute, at leading order in W , to the scattered power, spontaneous emission, and cross sections of extinction, absorption, and scattering. To this end, we expand the time propagator of Eq. (4) up to terms of order W^4 and represent diagrammatically the probabilities of the processes $\langle \Psi_n^f | \Psi_n(t) \rangle$, i.e., $P_n(t) = |\langle \Psi_n^f | \Psi_n(t) \rangle|^2$. In this expression the state $|\Psi_n(t)\rangle$ results from the evolution of one of the pure states $|\Psi_0\rangle_g$ or $|\Psi_0\rangle_e$ in a time interval t , $|\Psi_n(t)\rangle = \mathbb{U}(t) |\Psi_0\rangle_{g,e}$, and the state $|\Psi_n^f\rangle$ is that whose radiative content is to be computed for the calculation of the radiative power. Note that, in all the cases, the radiative content of $|\Psi_n^f\rangle$ differs from that of the pure states $|\Psi_0\rangle_{g,e}$ either in the net number of photons or in the frequency, momentum, and polarization of the photons. The corresponding processes are represented in Fig. 3 and are labeled with the subscript n . Since the illumination is continuous, we will be interested in steady processes for which we consider asymptotic times $\Gamma t \gg 1$.

A. Scattering

Scattering involves processes in which the atomic state in $|\Psi_n^f\rangle$ coincides with that in $|\Psi_n(0)\rangle$, but one of the probe photons in $|\Psi_n(0)\rangle$ is replaced in $|\Psi_n^f\rangle$ with a scattered photon of undefined frequency ω' , momentum \mathbf{k}' , and polarization ϵ' upon integration. That corresponds to diagrams (1) and (2) in Fig. 3, which represent scattering from the pure ground state and from the pure excited state, respectively, such that

$$\begin{aligned} |\Psi_1(0)\rangle &= |\Psi_0\rangle_g, & |\Psi_1^f\rangle &= \sum_{\mathbf{k}',\epsilon'} |(N-1)_{\mathbf{k},\epsilon}, 1_{\mathbf{k}',\epsilon'}; g\rangle, \\ |\Psi_2(0)\rangle &= |\Psi_0\rangle_e, & |\Psi_2^f\rangle &= \sum_{\mathbf{k}',\epsilon'} |(N-1)_{\mathbf{k},\epsilon}, 1_{\mathbf{k}',\epsilon'}; e\rangle. \end{aligned}$$

In the former case the emission of the scattered photon follows the absorption of the probe-field photon, whereas in the latter emission precedes absorption. It is important to note that, in the steady state and under continuous illumination $\Gamma t \gg 1$, the process of absorption of a probe-field photon in diagram (1) is followed without delay by the emission of a photon of undefined momentum. Thus, the emission process does not correspond to spontaneous emission but to continuous scattering [1]. Likewise, under continuous illumination, in diagram (2) the emission of a photon of undefined momentum is followed without delay by the absorption of a probe-field photon, resulting in continuous scattering. Things would be different if the probe field were a short pulse, in which case absorption would be followed by spontaneous emission. Therefore, in scattering processes the transition between atomic states is just transient and the scattered power is the time derivative of the EM energy,

$$\begin{aligned} \mathcal{W}_{\text{sc}} &= \sum_{n=1}^2 \frac{d}{dt} \langle \Psi_n(t) | \Psi_n^f \rangle \langle \Psi_n^f | H_{EM} | \Psi_n \rangle \langle \Psi_n^f | \Psi_n(t) \rangle \\ &= \frac{\hbar\omega\Omega_0^2\gamma_\omega}{4[(\omega - \omega_0)^2 + \Gamma^2/4]}, \quad \Gamma t \gtrsim 1, \end{aligned} \quad (14)$$

where $\gamma_\omega = \frac{-2\omega^2}{c^2\epsilon_0\hbar} \boldsymbol{\mu} \cdot \text{Im} \mathbb{G}(\mathbf{R}; \omega) \cdot \boldsymbol{\mu}$, $R \rightarrow 0^+$, and the scattering cross section reads

$$\sigma_{\text{sc}} = \frac{2\hbar\omega}{c\epsilon_0 E_0^2} \frac{d(P_1 + P_2)}{dt} = \frac{\mu_{\parallel}^2 \omega \gamma_\omega / 2\hbar\epsilon_0 c}{(\omega - \omega_0)^2 + \Gamma^2/4}, \quad (15)$$

where $\mu_{\parallel} = \boldsymbol{\mu} \cdot \boldsymbol{\epsilon}$. The reading of the contribution of diagrams (1) and (2) to \mathcal{W}_{sc} in terms of quantum operators and states is compiled in Appendix A 2.

B. Absorption, stimulated emission, and extinction

Generically, absorption processes are those in which states $|\Psi_n(0)\rangle$ and $|\Psi_n^f\rangle$ differ both in the atomic states and in the number of probe-field photons. They are represented by diagrams (3) and (4) of Fig. 3. In diagram (3) the atom at time t gets excited with respect to its initial state, while the EM state contains one probe photon less than the initial state. In diagram (4) the atom gets deexcited at time t while the EM

state contains one probe photon more than the initial state,

$$\begin{aligned} |\Psi_3(0)\rangle &= |\Psi_0\rangle_g, & |\Psi_3^f\rangle &= |(N-1)_{\mathbf{k},\epsilon}; e\rangle, \\ |\Psi_4(0)\rangle &= |\Psi_0\rangle_e, & |\Psi_4^f\rangle &= |(N+1)_{\mathbf{k},\epsilon}; g\rangle. \end{aligned}$$

The former process contributes to positive absorption, whereas the latter accounts for stimulated emission or negative absorption. In the steady state, under continuous illumination, the transition $g \leftrightarrow e$ induced by the potential W in either direction takes place at a constant rate Γ , as that is the coherence time sets by the pump. Thus, the rate at which an absorptive process takes place is Γ times the probability that such a process takes place for asymptotic times $\Gamma t \gg 1$. Also, since the states $|\Psi_0\rangle_g$ and $|\Psi_0\rangle_e$ are stationary, absorption is necessarily followed by processes that take the atomic state at time t back to the atomic state at time 0. In particular, the state e decays into g either emitting a scattered photon of frequency ω according to diagram (1) in Fig. 3 or by non-radiative means. Therefore, in order not to double count the probability of radiative decay, the contribution of diagram (1) must be subtracted from that of diagram (3) in the calculation of net absorption, resulting in nonradiative absorption only. Likewise, the state g at time t in diagram (4) ends up transiting to state e under the action of the pump which, according to Fig. 2(a), is accompanied by the spontaneous emission of photons of frequency approximately equal to $\omega_u - \omega_0$. Since no other radiative processes are involved there, no double counting is associated with the probability of the process in diagram (4).

Thus, the power absorbed by the system is written as

$$\begin{aligned} \mathcal{W}_{\text{abs}} &= \Gamma \sum_{n=3}^4 [\langle \Psi_n(0) | H_{EM} | \Psi_n(0) \rangle - \langle \Psi_n(t) | \Psi_n^f \rangle] \\ &\quad \times \langle \Psi_n^f | H_{EM} | \Psi_n^f \rangle \langle \Psi_n^f | \Psi_n(t) \rangle - \frac{d}{dt} \langle \Psi_1(t) | \Psi_1^f \rangle \\ &\quad \times \langle \Psi_1^f | H_{EM} | \Psi_1^f \rangle \langle \Psi_1^f | \Psi_1(t) \rangle \\ &= \frac{\hbar\omega\Omega_0^2(\gamma - \mathcal{P} - \frac{\gamma}{\Gamma}\gamma_\omega)}{4[(\omega - \omega_0)^2 + \Gamma^2/4]} \\ &= \frac{\hbar\omega\Omega_0^2(\frac{\gamma}{\Gamma}\gamma_{nr} - \frac{\mathcal{P}}{\Gamma}\mathcal{P})}{4[(\omega - \omega_0)^2 + \Gamma^2/4]}, \quad \Gamma t \gtrsim 1, \end{aligned} \quad (16)$$

where the time-derivative term with a minus sign in front stems from the subtraction of the scattered power from the pure ground state. As for the absorption cross section,

$$\begin{aligned} \sigma_{\text{abs}} &= \frac{2\hbar\omega}{c\epsilon_0 E_0^2} \left[\Gamma(P_3 - P_4) - \frac{dP_1}{dt} \right] \\ &\simeq \frac{\mu_{\parallel}^2 \omega (\frac{\gamma}{\Gamma}\gamma_{nr} - \frac{\mathcal{P}}{\Gamma}\mathcal{P}) / 2\hbar\epsilon_0 c}{(\omega - \omega_0)^2 + \Gamma^2/4}, \end{aligned} \quad (17)$$

where the minus sign in front of P_4 accounts for the negative nature of the absorption associated with stimulated emission. The reading of the contributions of diagrams (3) and (4) to \mathcal{W}_{abs} are compiled in Appendix A 2. Finally, the extinction

cross section is the addition of σ_{sc} and σ_{abs} , which yields

$$\begin{aligned}\sigma_{ext} &\simeq \frac{\mu_{\parallel}^2 \omega (\gamma_{\omega} + \frac{\gamma}{\Gamma} \gamma_{nr} - \frac{\mathcal{P}}{\Gamma} \mathcal{P}) / 2\hbar\epsilon_0 c}{(\omega - \omega_0)^2 + \Gamma^2/4} \\ &= \frac{\mu_{\parallel}^2 \omega [\gamma - \frac{\mathcal{P}}{\Gamma} (\gamma_{nr} + \mathcal{P})] / 2\hbar\epsilon_0 c}{(\omega - \omega_0)^2 + \Gamma^2/4}.\end{aligned}\quad (18)$$

C. Spontaneous emission

Finally, spontaneous emission, up to terms of order Ω_0^2/Γ^2 , corresponds to the processes depicted by diagrams (5)–(7) in Fig. 3. In all of them the atom transits from the excited state at time 0 to the ground state at time t , and $|\Psi_n^f\rangle$ contains the same number of probe-field photons as $|\Psi_n(0)\rangle$, plus one more photon of undefined frequency, momentum, and polarization upon integration,

$$|\Psi_{5,6,7}(0)\rangle = |\Psi_0\rangle_e, \quad |\Psi_{5,6,7}^f\rangle = \sum_{\mathbf{k}, \epsilon} |N_{\mathbf{k}, \epsilon}, 1_{\mathbf{k}', \epsilon'}; g\rangle.$$

Diagram (5) is similar to those for the natural decay rate in the absence of the probe field in Fig. 2(b), γ_0 , but for the fact that the pump enhances the effective incoherence rate and thus the width of the emission line. On the other hand, diagrams (6) and (7) depict the influence of the probe field on spontaneous emission. Note that, in contrast to the scattering diagram (2), a probe-field photon in the final state is not effectively absorbed, as it reappears in the final state. As with absorption, under steady conditions, the rate at which the spontaneous emission processes take place is Γ times their probabilities for asymptotic times $\Gamma t \gg 1$. Spontaneous emission is inherently incoherent and its power reads

$$\begin{aligned}\mathcal{W}_{inc} &= \Gamma \sum_{n=5}^7 [\langle \Psi_n(t) | \Psi_n^f \rangle \langle \Psi_n^f | H_{EM} | \Psi_n^f \rangle \langle \Psi_n^f | \Psi_n(t) \rangle \\ &\quad - \langle \Psi_n(0) | H_{EM} | \Psi_n(0) \rangle] \\ &= \frac{\mathcal{P}}{\Gamma} \left\{ \hbar\omega_0\gamma_0 - \frac{\Omega_0^2\Gamma^2/8}{[(\omega - \omega_0)^2 + \Gamma^2/4]^2} \right. \\ &\quad \left. \times \left[\hbar\omega\gamma_{\omega} - \frac{\hbar\omega_0\gamma_0}{2} + \frac{2\hbar\omega_0\gamma_0(\omega - \omega_0)^2}{\Gamma^2} \right] \right\} \\ &\simeq \frac{\hbar\omega_0\gamma_0\mathcal{P}}{\Gamma} \left[1 - \frac{\Omega_0^2\Gamma^2/16}{[(\omega - \omega_0)^2 + \Gamma^2/4]^2} \right], \quad \Gamma t \gtrsim 1.\end{aligned}\quad (19)$$

Note that the quasisonant probe field in diagrams (6) and (7) generates resonances at ω in addition to those at ω_0 in the spectrum of spontaneous emission. Further, in the limit $|\omega - \omega_0|/\Gamma \rightarrow 0$, we obtain a probe-field-corrected spontaneous emission rate $\mathcal{P}\gamma_0(1 - \Omega_0^2/\Gamma^2)/\Gamma$. The readings of the contributions of diagrams (5)–(7) to \mathcal{W}_{inc} are compiled in Appendix A 2.

IV. ENERGETICS: BALANCE BETWEEN GAIN AND LOSS

Regarding the energetic content of the radiative processes, the interpretation is as follows. From the expression on the right-hand side of the first equality in Eq. (18) for the extinction cross section we read that, in addition to the scattering

term proportional to γ_{ω} , the nonradiative dissipative term, proportional to the population rate of the ground state $\gamma\gamma_{nr}/\Gamma$, accounts for positive losses, and the negative term, proportional to the population rate of the excited state $-\mathcal{P}^2/\Gamma$, stems from the stimulated emission fed by the pump. On the other hand, from the expression on the right-hand side of the second equality in Eq. (18), we read that the net action of the pump on the probe field is that of reducing its extinction in an amount proportional to $-\mathcal{P}(\mathcal{P} + \gamma_{nr})/\Gamma$. That is, the excited-state population contributes positively to probe-field radiation through stimulated emission and reduces the nonradiative losses associated with the transition $e \rightarrow g$ after the transient excitation caused by the probe field from the state g to e . On top of that, the incoherent power of Eq. (19) is proportional to the population rate of the excited state too. In summary, Eq. (18) for σ_{ext} differs from that of an atom in its ground state not only in the enhancement of its linewidth and the attenuation of its spectral amplitude, but also in the diminishing of nonradiative losses and in the gain provided by stimulated emission. Both effects are proportional to the population of the excited state, being the associated energy supplied by the pump. Finally, the incoherent power of Eq. (19) associated with the spontaneous decay from the excited to the ground state is supplied by the pump too.

We finalize this section with the graphical representation of the cross sections in terms of the parameters of gains and losses, i.e., \mathcal{P} and γ , respectively. From the expressions of Eqs. (15), (17), and (18) for σ_{sc} , σ_{abs} , and σ_{ext} we note that the linewidth of all the spectra increases with gains and losses in the same manner, $\Gamma = \gamma + \mathcal{P}$, while the spectral amplitudes decrease. However, for the case that either the nonradiative decay rate or the pump rate becomes dominant, the scaling behaviors of the cross sections differ from one another. That is, for $\gamma_{nr} \gg \gamma_{\omega}$, \mathcal{P} , we find for scattering $\sigma_{sc} \sim 1/\gamma_{nr}^2$, while for absorption and extinction we get $\sigma_{abs}, \sigma_{ext} \sim 1/\gamma_{nr}$. Likewise, for $\mathcal{P} \gg \gamma_{nr}, \gamma_{\omega}$, we have $\sigma_{sc} \sim 1/\mathcal{P}^2$ and $\sigma_{abs}, \sigma_{ext} \sim 1/\mathcal{P}$. Besides, while scattering is hardly affected by the relationship between gains and losses, absorption and extinction are. In particular, absorption vanishes for $\mathcal{P} = \sqrt{\gamma_{nr}^2 + \gamma_{nr}\gamma_{\omega}}$, while extinction does so for $\mathcal{P} = [\gamma_{\omega} + \sqrt{4\gamma_{nr}^2 + 8\gamma_{nr}\gamma_{\omega} + 5\gamma_{\omega}^2}]/2$. The latter equality determines the balance between gains and losses which, in an effective manner, is a necessary condition for \mathcal{PT} symmetry [25,33,36]. In particular, for $\gamma_{nr} \ll \gamma_{\omega} \simeq \gamma_0$, null extinction holds for $\mathcal{P} \simeq \gamma_0(1 + \sqrt{5})/2$.

In Fig. 4 we represent the scattering, absorption, and extinction cross sections for different values of the pump rate. The cross sections are expressed in units of $\sigma_{sc}(\omega = \omega_0, \Gamma = \gamma_0) \equiv \sigma_0 = 2\omega_0\mu_{\parallel}^2/c\epsilon_0\hbar\gamma_0$, and the gain and loss rates are given in units of γ_0 . In Fig. 5 we represent the cross sections at exact resonance $\omega = \omega_0$ in terms of the pump rate at a fixed value of the nonradiative decay rate $\gamma_{nr} = \gamma_0/5$. Extinction becomes negative for $\mathcal{P} \gtrsim 1.8\gamma_0$.

V. DISCUSSION

A. Unitarity and energy balance

On the one hand, our Hamiltonian approach allows us to keep track of the atomic dynamics as well as all the radiative

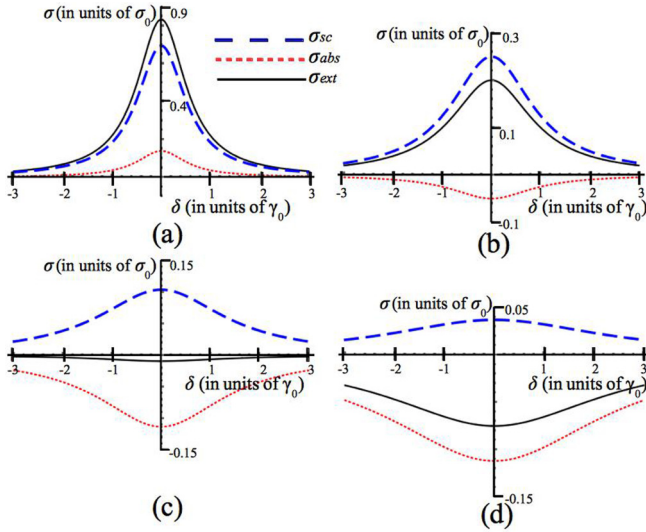


FIG. 4. Graphical representation of the scattering, absorption, and extinction cross sections for a fixed value of the nonradiative decay rate $\gamma_{nr} = \gamma_0/5$ and different values of the pump rate (a) $\mathcal{P} = 0$, (b) $\mathcal{P} = 0.8\gamma_0$, (c) $\mathcal{P} = 1.9\gamma_0$, and (d) $\mathcal{P} = 4\gamma_0$. Cross sections are expressed in units of $\sigma_0 = 2\omega_0\mu_{\parallel}^2/c\epsilon_0\hbar\gamma_0$. The detuning $\delta = \omega - \omega_0$ is given in units of γ_0 .

time processes. On the other hand, incoherent processes are accounted for in an effective manner that should be consistent with unitarity. This means that, starting with the normalized mixed steady state defined as the incoherent superposition of the pure states in Eq. (13), the addition of the time derivatives of the probabilities of all the processes which take the system to a state different from $|\Psi_0\rangle_{g,e}$, $P_{\Psi_0 \rightarrow \Psi_0}$, and those which take it back to $|\Psi_0\rangle_{g,e}$, $P_{\Psi_0 \rightarrow \Psi_0}$, must be identically zero. This should be the case at all orders. In particular, at the order Ω_0^2/Γ , the time derivative of the probabilities of the radiative processes computed in the preceding section amounts to

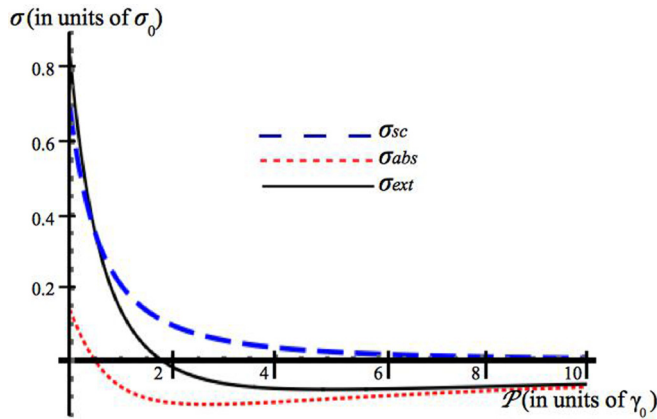


FIG. 5. Graphical representation of the scattering, absorption, and extinction cross sections for a fixed value of the nonradiative decay rate $\gamma_{nr} = \gamma_0/5$ as a function of the pump rate \mathcal{P} . Cross sections are expressed in units of $\sigma_0 = 2\omega_0\mu_{\parallel}^2/c\epsilon_0\hbar\gamma_0$. The pump rate is given in units of γ_0 .

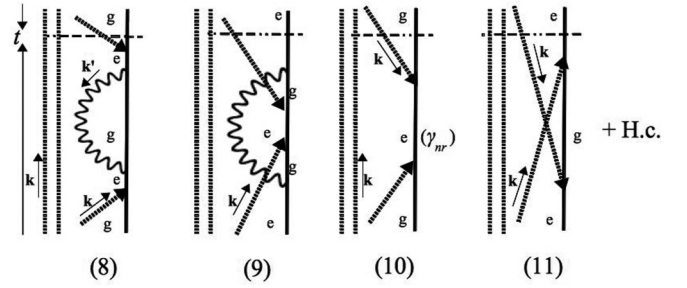


FIG. 6. Diagrammatic representation of the four processes that, together with their Hermitian conjugate versions (H.c.), contribute at leading order to $P_{\Psi_0 \rightarrow \Psi_0}$ and thus to the renormalization of the pure steady states $|\Psi_0\rangle_{g,e}$. As explained in the text, since $|\Psi_0\rangle_{g,e}$ are already normalized, the addition of the probabilities of these processes to those of the processes depicted in Fig. 3 vanishes identically.

$$\begin{aligned} & \frac{d}{dt} P_{\Psi_0 \rightarrow \Psi_0} |_{O(\Omega_0^2/\Gamma)} \\ &= \frac{d}{dt} (P_1 + P_2) + \Gamma(P_3 + P_4 + P_6 + P_7) \\ &\simeq \frac{\Omega_0^2(\gamma + \mathcal{P} + \frac{\mathcal{P}}{\Gamma}\gamma\omega - \frac{\mathcal{P}}{\Gamma}\gamma_0)}{4[(\omega - \omega_0)^2 + \Gamma^2/4]} \simeq \Omega_0^2/\Gamma, \quad |\omega - \omega_0| \ll \Gamma, \end{aligned} \quad (20)$$

whereas the processes of Fig. 6 give rise to an effective renormalization of the states $|\Psi_0\rangle_{g,e}$ proportional to Ω_0^2 ,

$$\begin{aligned} & \frac{d}{dt} P_{\Psi_0 \rightarrow \Psi_0} |_{O(\Omega_0^2/\Gamma)} = 2 \frac{d}{dt} (P_8 + P_{10} + P_{11}) \\ &\simeq \frac{-\Omega_0^2(\gamma + \mathcal{P})}{4[(\omega - \omega_0)^2 + \Gamma^2/4]} \simeq -\Omega_0^2/\Gamma, \quad |\omega - \omega_0| \ll \Gamma, \end{aligned} \quad (21)$$

yielding $\frac{d}{dt} (P_{\Psi_0 \rightarrow \Psi_0} + P_{\Psi_0 \rightarrow \Psi_0}) |_{O(\Omega_0^2/\Gamma)} = 0$, as expected. Note that the contributions of diagrams (5) and (9) have been discarded in Eqs. (20) and (21), respectively, as they are of orders γ_0 and $\gamma_0\Omega_0^2/\omega^2$ instead.

B. Semiclassical computation of the coherent scattered power

In semiclassical approaches based on the density-functional formalism [21,28,29] and linear response theory [12,25], it is customary to refer to coherent scattered power as that in phase with the steady oscillations of the expectation value of the atomic dipole moment $\langle \mathbf{d}(t) \rangle$. In order to interpret the coherent power in terms of our Hamiltonian approach, let us consider the probe field as classical. The Hamiltonian of the interaction between the atomic dipole and the probe field comes to depend on time and is written $W = \tilde{W}(t) + \tilde{W}^\dagger(t)$, with $\tilde{W} = \mathbf{d} \cdot \epsilon E_0 e^{-i\omega t} / 2i$, and the probe-field photons are to be dropped from the steady state of the system in Eq. (13), which becomes now an incoherent superposition of the states $|\tilde{\Psi}_0\rangle_g = \sqrt{\gamma/\Gamma}|g\rangle$ and $|\tilde{\Psi}_0\rangle_e = \sqrt{\mathcal{P}/\Gamma}|e\rangle$. Next, let us use a complex-valued representation for the expectation values such that the physical values correspond to their real parts. Applying standard time-dependent perturbation theory, the complex-valued averaged expectation value of the total dipole

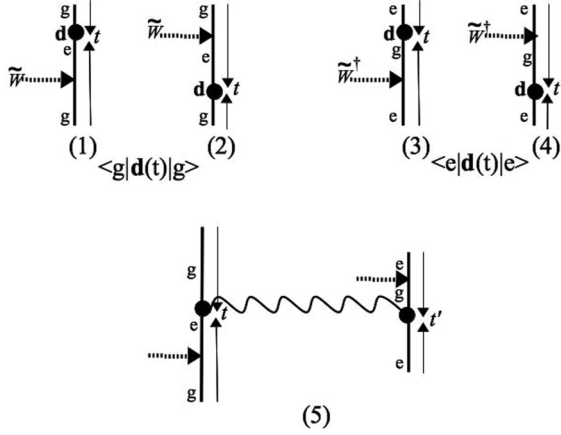


FIG. 7. Diagrammatic representation of the four processes that contribute, at leading order, to the expectation values $\langle g|\mathbf{d}(t)|g\rangle$ [(1) and (2)] and $\langle e|\mathbf{d}(t)|e\rangle$ [(3) and (4)]. Dashed arrows depicts the action of the interaction potential \tilde{W} , while black closed circles represent the action of the dipole moment operator at the observation time t . In diagram (5) we represent one of the terms of \mathcal{W}_{coh} in Eq. (25), proportional to $\gamma\mathcal{P}/\Gamma^2$, where several expectation values are combined. The wavy line represents the time propagator of the electric field.

moment reads, in the steady state $\Gamma t \gg 1$,

$$\begin{aligned} \langle \mathbf{d}(t) \rangle &= \frac{\gamma}{\Gamma} \langle g|\mathbf{d}(t)|g\rangle + \frac{\mathcal{P}}{\Gamma} \langle e|\mathbf{d}(t)|e\rangle \\ &= \frac{\mathcal{P} - \gamma}{\Gamma} \frac{ie^{-i\omega t} \Omega_0 \boldsymbol{\mu}}{\omega - \omega_0 + i\Gamma/2} \equiv \langle \mathbf{d}(\omega) \rangle e^{-i\omega t}, \end{aligned} \quad (22)$$

where the two terms on the right-hand side of the first equality are represented by diagrams (1) and (4) of Fig. 7 and off-resonant components have been discarded. From Eq. (22) the effective polarizability can be readily identified with [28]

$$\alpha(\omega) = \frac{\mathcal{P} - \gamma}{\Gamma} \frac{\boldsymbol{\mu} \boldsymbol{\mu}}{\hbar(\omega - \omega_0 + i\Gamma/2)} \quad (23)$$

such that $\langle \mathbf{d}(\omega) \rangle = \alpha(\omega) \cdot \boldsymbol{\epsilon} E_0$. Note that the effective polarizability vanishes for equal population rates $\mathcal{P} = \gamma$ and so does the expectation value of the dipole moment.

Further, applying semiclassical linear response theory, the complex-valued coherent field created at position \mathbf{r} and time t by the atomic dipole reads

$$\mathbf{E}(\mathbf{r}, \omega) = -k^2 \epsilon_0^{-1} \mathbb{G}(\mathbf{r} - \mathbf{r}_A; \omega) \langle \mathbf{d}(\omega) \rangle, \quad (24)$$

where $\mathbb{G}(\mathbf{r}, \mathbf{r}_A, \omega)$ is given in Eq. (3), which is the retarded time Fourier transform of the vacuum commutator of the electric field [11] $\mathbb{G}(\mathbf{r} - \mathbf{r}_A; t - t') \propto i\langle 0 | [\mathbf{E}(\mathbf{r}, t), \mathbf{E}(\mathbf{r}_A, t')] | 0 \rangle$, $t \geq t'$. Correspondingly, the power emitted by the coherent dipole is defined as the time-average rate of the interaction of the induced dipole with its own electric field [12],

$$\begin{aligned} \mathcal{W}_{\text{coh}} &= \frac{-\omega}{2} \text{Im} \{ \langle \mathbf{d}(\omega) \rangle \cdot \mathbf{E}^*(\mathbf{r}_A, \omega) \} \\ &= -\frac{\omega^3}{c^2 \epsilon_0} \langle \mathbf{d}(\omega) \rangle \cdot \text{Im} \mathbb{G}(\mathbf{R}; \omega) \cdot \langle \mathbf{d}^*(\omega) \rangle \\ &= \frac{-(\mathcal{P} - \gamma)^2}{\Gamma^2} \frac{\omega^3 \Omega_0^2 \boldsymbol{\mu} \cdot \text{Im} \mathbb{G}(\mathbf{R}; \omega) \cdot \boldsymbol{\mu}}{2c^2 \epsilon_0 [(\omega - \omega_0)^2 + \Gamma^2/4]}, \quad R \rightarrow 0^+, \end{aligned} \quad (25)$$

which, oddly enough, vanishes for $\mathcal{P} = \gamma$. Our fully Hamiltonian and quantum computation of Eqs. (A3), (A4), and (14) yields instead

$$\mathcal{W}_{\text{sc}} = -\frac{\omega^3 \Omega_0^2 \boldsymbol{\mu} \cdot \text{Im} \mathbb{G}(\mathbf{R}; \omega) \cdot \boldsymbol{\mu}}{2c^2 \epsilon_0 [(\omega - \omega_0)^2 + \Gamma^2/4]}, \quad R \rightarrow 0^+, \quad (26)$$

which differs from the semiclassical calculation of \mathcal{W}_{coh} in the factor $(\mathcal{P} - \gamma)^2/\Gamma^2$. More importantly, we note that while \mathcal{W}_{sc} corresponds to the time derivative of the quantum expectation value of the electromagnetic energy according to Eq. (14), \mathcal{W}_{coh} in Eq. (25) does not correspond to the quantum expectation value of any observable but to the product of several expectation values inspired by classical formulas [12]. The fact that no term within \mathcal{W}_{sc} is quadratic in the population rates [see Eqs. (A3) and (A4) in Appendix A2] suggests that the semiclassical calculation is not a good approximation. Hence, the term in \mathcal{W}_{coh} proportional to $\gamma\mathcal{P}/\Gamma^2$ is the result of the coupling between ${}_g\langle \tilde{\Psi}_0 | \mathbf{d}(t) | \tilde{\Psi}_0 \rangle_g$ and ${}_e\langle \tilde{\Psi}_0 | \mathbf{d}(t) | \tilde{\Psi}_0 \rangle_e$, which are mutually incoherent indeed (see Fig. 7).

VI. CONCLUSION

Based on QED Hamiltonian perturbation theory, we have developed a wave-function approach to characterize the optical response of a three-level atom subjected to an incoherent pump and illuminated by a continuous, weak, and quasisonant probe field. In the first place, we integrate adiabatically the dynamics of the upper atomic state and incorporate the incoherent dynamics associated with the pump and the spontaneous emission in exponentially attenuating factors which accompany the Hermitian time propagator. We have verified that our approach is compatible with unitarity.

We have identified all the radiative processes which contribute to scattering, absorption, and spontaneous emission and have depicted them diagrammatically. We have found that, generically, the pump enhances the linewidth and attenuates the amplitude of the spectra. In addition, extinction differs from that of a free atom in its ground state in the diminishing of the nonradiative losses and in the compensation of the losses by stimulated emission [Eq. (18)]. Both effects are proportional to the steady population of the excited state, being the associated energy supplied by the pump. Finally, the incoherent power of Eq. (19), associated with the spontaneous decay from the excited to the ground state, is supplied by the pump too.

Extinction becomes negative for sufficiently strong pumping rate, vanishing for $\mathcal{P} = [\gamma_\omega + \sqrt{4\gamma_{nr}^2 + 8\gamma_{nr}\gamma_\omega + 5\gamma_\omega^2}]/2$. At this point gains and losses compensate, satisfying one of the necessary conditions for \mathcal{PT} symmetry in an optical system.

In passing, we have shown that a semiclassical calculation fails in providing a good estimate of the scattered power.

Our development paves the way for its extension to many-atom systems with gains and losses. In this respect, prospective work could characterize the optical response of a pair of identical atoms, with one of them continuously pumped, in order to study its \mathcal{PT} -symmetry properties.

ACKNOWLEDGMENTS

Helpful discussions with Alejandro Manjavacas and Julio Sánchez-Cánovas are gratefully acknowledged. This work

was sponsored by Junta de Castilla y León through Grants No. VA137G18 and No. BU229P18.

APPENDIX: DIAGRAM READING AND QUANTUM EXPRESSIONS

In this Appendix we compile the complete expressions of the quantum processes represented diagrammatically in the main text, in terms of quantum states and operators.

1. Incoherent transition rates

The expression corresponding to the diagrams of Fig. 2(a) for the incoherent pump transition rate of Eq. (5) reads

$$\begin{aligned}
 \mathcal{P} &= \frac{d}{dt} \sum_{\mathbf{k}', \epsilon'} \{ \dots \}^\dagger \cdot \left\{ \hbar^{-2} \int_0^t d\tau \int_0^\tau d\tau' \mathbb{U}_0(t-\tau) |1_{\mathbf{k}', \epsilon'}, (N-1)_{\mathbf{k}_p, \epsilon_p}; e\rangle \langle 1_{\mathbf{k}', \epsilon'}, (N-1)_{\mathbf{k}_p, \epsilon_p}; e| \mathbf{d} \right. \\
 &\quad \cdot \mathbf{E}_{\mathbf{k}', \epsilon'}^{(-)}(\mathbf{r}_A) | (N-1)_{\mathbf{k}_p, \epsilon_p}; u \rangle \langle (N-1)_{\mathbf{k}_p, \epsilon_p}; u | \mathbb{U}_0(\tau-\tau') e^{-\gamma_u(\tau-\tau')/2} | (N-1)_{\mathbf{k}_p, \epsilon_p}; u \rangle \\
 &\quad \left. \times \langle (N-1)_{\mathbf{k}_p, \epsilon_p}; u | \mathbf{d} \cdot \mathbf{E}(\mathbf{r}_A) | N_{\mathbf{k}_p, \epsilon_p}; g \rangle \langle N_{\mathbf{k}_p, \epsilon_p}; g | \mathbb{U}_0(\tau') | N_{\mathbf{k}_p, \epsilon_p}; g \rangle \right\} \\
 &= \Omega_p^2 \text{Re} \frac{d}{dt} \int_0^\infty \frac{-dk' ck'^2}{\epsilon_0 \hbar \pi} \boldsymbol{\mu} \cdot \text{Im} \mathbb{G}(\mathbf{R}; k') \cdot \boldsymbol{\mu} \left| \int_0^t d\tau e^{-i(t-\tau)(\omega' + \omega_0)} \int_0^\tau d\tau' e^{-i(\tau-\tau')\omega_u} e^{-(\tau-\tau')\gamma_u/2} e^{-i\tau'\omega_p} \right|^2 \\
 &\simeq \frac{\Omega_p^2 c}{2\pi \epsilon_0 \hbar} \text{Re} \int_0^\infty dk' i \frac{k'^2 \boldsymbol{\mu} \cdot \text{Im} \mathbb{G}(\mathbf{R}; k') \cdot \boldsymbol{\mu} e^{it(\omega' - \omega_u + \omega_0)}}{(\omega' - \omega_u + \omega_0)[(\omega' - \omega_u + \omega_0)^2 + \gamma_u^2/4]}, \quad \gamma_u t \gg 1, R \rightarrow 0^+, \tag{A1}
 \end{aligned}$$

where $\{ \dots \}^\dagger$ is the conjugate transpose of the state whose expression appears within curly brackets on its right-hand side after the dot product symbol. The exponential factor $e^{-\gamma_u(\tau-\tau')/2}$ stems from the addition of all the one-photon emission-reabsorption intermediate processes in Fig. 2(a), and the rapid decay from u to e is accounted for by the condition $\gamma_u t \gg 1$. As for the diagrams of Fig. 2(b) corresponding to the spontaneous emission rate from state e , they read

$$\begin{aligned}
 \gamma_0 &= \frac{d}{dt} \sum_{\mathbf{k}', \epsilon'} \{ \dots \}^\dagger \cdot \left\{ \hbar^{-1} \int_0^t d\tau \mathbb{U}_0(t-\tau) |1_{\mathbf{k}', \epsilon'}, N_{\mathbf{k}_p, \epsilon_p}; g\rangle \langle 1_{\mathbf{k}', \epsilon'}, N_{\mathbf{k}_p, \epsilon_p}; g| \mathbf{d} \cdot \mathbf{E}_{\mathbf{k}', \epsilon'}^{(-)}(\mathbf{r}_A) | N_{\mathbf{k}_p, \epsilon_p}; e \rangle \langle N_{\mathbf{k}_p, \epsilon_p}; e | \mathbb{U}_0(\tau) e^{-\gamma\tau/2} | N_{\mathbf{k}_p, \epsilon_p}; e \rangle \right\} \\
 &= \frac{d}{dt} \int_0^\infty \frac{-dk' ck'^2}{\epsilon_0 \hbar \pi} \boldsymbol{\mu} \cdot \text{Im} \mathbb{G}(\mathbf{R}; k') \cdot \boldsymbol{\mu} \left| \int_0^t d\tau e^{-i(t-\tau)\omega'} e^{-i\tau\omega_0} e^{-\tau\gamma/2} \right|^2 \\
 &\simeq \int_0^\infty \frac{dk' c}{\epsilon_0 \hbar \pi} \frac{k'^2 \boldsymbol{\mu} \cdot \text{Im} \mathbb{G}(\mathbf{R}; k') \cdot \boldsymbol{\mu} [e^{it(\omega' - \omega_0)}[\gamma/2 - i(\omega' - \omega_0)] + e^{-it(\omega' - \omega_0)}[\gamma/2 + i(\omega' - \omega_0)] - \gamma]}{(\omega' - \omega_0)^2 + \gamma^2/4}, \quad \gamma t \ll 1, R \rightarrow 0^+, \tag{A2}
 \end{aligned}$$

where the exponential factor $e^{-\gamma\tau/2}$ stems from the addition of all the explicit one-photon emission-reabsorption intermediate processes as well as the implicit nonradiative decay channels in Fig. 2(b). Slow decay is implicit in the condition $\gamma t \ll 1$.

2. Scattered, absorbed, and incoherent emission powers

The expressions of the scattered power corresponding to diagrams (1) and (2) in Fig. 3 according to Eq. (14) read, respectively,

$$\begin{aligned}
 \mathcal{W}^{(1)} &= \frac{d}{dt} \langle \Psi_1(t) | \Psi_n^f \rangle \langle \Psi_1^f | H_{EM} | \Psi_1^f \rangle \langle \Psi_1^f | \Psi_1(t) \rangle \\
 &= \frac{\gamma}{\Gamma} \frac{d}{dt} \sum_{\mathbf{k}', \epsilon'} \hbar \omega' \{ \dots \}^\dagger \cdot \left\{ \hbar^{-2} \int_0^t d\tau \int_0^\tau d\tau' a_{\mathbf{k}', \epsilon'} \mathbb{U}_0(t-\tau) |1_{\mathbf{k}', \epsilon'}, (N-1)_{\mathbf{k}, \epsilon}; g\rangle \langle 1_{\mathbf{k}', \epsilon'}, (N-1)_{\mathbf{k}, \epsilon}; e| \mathbf{d} \right. \\
 &\quad \cdot \mathbf{E}_{\mathbf{k}', \epsilon'}^{(-)}(\mathbf{r}_A) | (N-1)_{\mathbf{k}, \epsilon}; e \rangle \langle (N-1)_{\mathbf{k}, \epsilon}; e | \mathbb{U}_0(\tau-\tau') e^{-\Gamma(\tau-\tau')/2} | (N-1)_{\mathbf{k}, \epsilon}; e \rangle \langle (N-1)_{\mathbf{k}, \epsilon}; e | \mathbf{d} \\
 &\quad \left. \cdot \mathbf{E}(\mathbf{r}_A) | N_{\mathbf{k}, \epsilon}; g \rangle \langle N_{\mathbf{k}, \epsilon}; g | \mathbb{U}_0(\tau') | N_{\mathbf{k}, \epsilon}; g \rangle \right\} \\
 &= \frac{\Omega_0^2 \gamma}{\Gamma} \text{Re} \frac{d}{dt} \int_0^\infty \frac{-dk' c^2 k'^3}{\epsilon_0 \pi} \boldsymbol{\mu} \cdot \text{Im} \mathbb{G}(\mathbf{R}; k') \cdot \boldsymbol{\mu} \left| \int_0^t d\tau e^{-i(t-\tau)\omega'} \int_0^\tau d\tau' e^{-i(\tau-\tau')\omega_0} e^{-(\tau-\tau')\Gamma/2} e^{-i\tau'\omega} \right|^2
 \end{aligned}$$

$$\begin{aligned}
&\simeq \frac{-\Omega_0^2 c^2 \gamma}{2\pi \epsilon_0 \Gamma} \text{Im} \int_0^\infty dk' \frac{k'^3 \boldsymbol{\mu} \cdot \text{Im} \mathbb{G}(\mathbf{R}; k') \cdot \boldsymbol{\mu} e^{it(\omega' - \omega)}}{(\omega' - \omega)(\omega' - \omega_0 - i\Gamma/2)(\omega - \omega_0 + i\Gamma/2)} \\
&= \frac{-\Omega_0^2 c^2 \gamma}{4\epsilon_0 \Gamma} \frac{2\omega^3 \boldsymbol{\mu} \cdot \text{Im} \mathbb{G}(\mathbf{R}; \omega) \cdot \boldsymbol{\mu}}{(\omega - \omega_0)^2 + \Gamma^2/4}, \quad \Gamma t \gg 1, R \rightarrow 0^+,
\end{aligned} \tag{A3}$$

$$\begin{aligned}
\mathcal{W}^{(2)} &= \frac{d}{dt} \langle \Psi_2(t) | \Psi_2^f \rangle \langle \Psi_2^f | H_{EM} | \Psi_2^f \rangle \langle \Psi_2^f | \Psi_2(t) \rangle \\
&= \frac{\mathcal{P}}{\Gamma} \frac{d}{dt} \sum_{\mathbf{k}', \epsilon'} \hbar \omega' \{ \dots \}^\dagger \cdot \left\{ \hbar^{-2} \int_0^t d\tau \int_0^\tau d\tau' a_{\mathbf{k}', \epsilon'} \mathbb{U}_0(t - \tau) | 1_{\mathbf{k}', \epsilon'}, (N-1)_{\mathbf{k}, \epsilon}; e \rangle \langle 1_{\mathbf{k}', \epsilon'}, (N-1)_{\mathbf{k}, \epsilon}; e | \mathbf{d} \right. \\
&\quad \cdot \mathbf{E}(\mathbf{r}_A) | 1_{\mathbf{k}', \epsilon'}, N_{\mathbf{k}, \epsilon}; g \rangle \langle 1_{\mathbf{k}', \epsilon'}, N_{\mathbf{k}, \epsilon}; g | \mathbb{U}_0(\tau - \tau') | 1_{\mathbf{k}', \epsilon'}, N_{\mathbf{k}, \epsilon}; g \rangle \langle \mathbf{k}', N_{\mathbf{k}, \epsilon}; g | \mathbf{d} \\
&\quad \left. \cdot \mathbf{E}_{\mathbf{k}', \epsilon'}^{(-)}(\mathbf{r}_A) | N_{\mathbf{k}, \epsilon}; e \rangle \langle N_{\mathbf{k}, \epsilon}; e | \mathbb{U}_0(\tau') | N_{\mathbf{k}, \epsilon}; e \rangle \right\} \\
&= \frac{\Omega_0^2 \mathcal{P}}{4\Gamma} \frac{d}{dt} \int_0^\infty \frac{-dk' c^2 k'^3}{\epsilon_0 \pi} \boldsymbol{\mu} \cdot \text{Im} \mathbb{G}(\mathbf{R}; k') \cdot \boldsymbol{\mu} \left| \int_0^t d\tau e^{-i(t-\tau)(\omega' + \omega_0)} \int_0^\tau d\tau' e^{-i(\tau-\tau')(\omega' + \omega)} e^{-(\tau-\tau')\Gamma/2} e^{-i\tau'(\omega_0 + \omega)} \right|^2 \\
&\simeq \frac{-\Omega_0^2 c^2 \mathcal{P}}{2\pi \epsilon_0 \Gamma} \text{Im} \int_0^\infty dk' \frac{k'^3 \boldsymbol{\mu} \cdot \text{Im} \mathbb{G}(\mathbf{R}; k') \cdot \boldsymbol{\mu} e^{it(\omega' - \omega)}}{(\omega' - \omega)(\omega' - \omega_0 - i\Gamma/2)(\omega - \omega_0 + i\Gamma/2)} \\
&= \frac{-\Omega_0^2 \mathcal{P}}{4c^2 \epsilon_0 \Gamma} \frac{2\omega^3 \boldsymbol{\mu} \cdot \text{Im} \mathbb{G}(\mathbf{R}; \omega) \cdot \boldsymbol{\mu}}{(\omega - \omega_0)^2 + \Gamma^2/4}, \quad \Gamma t \gg 1, R \rightarrow 0^+.
\end{aligned} \tag{A4}$$

The contributions of diagrams (3) and (4) of Fig. 3 to the power absorbed by the atom according to Eq. (16) are, respectively,

$$\begin{aligned}
\mathcal{W}^{(3)} &= \Gamma \left[\langle \Psi_3(0) | H_{EM} | \Psi_3(0) \rangle - \langle \Psi_3(t) | \Psi_3^f \rangle \langle \Psi_3^f | H_{EM} | \Psi_3^f \rangle \langle \Psi_3^f | \Psi_3(t) \rangle \right] \\
&= \Gamma \frac{\gamma}{\Gamma} \sum_{\mathbf{k}, \epsilon} \langle N_{\mathbf{k}, \epsilon}; g | \hbar \omega' a_{\mathbf{k}', \epsilon}^\dagger a_{\mathbf{k}', \epsilon} | N_{\mathbf{k}, \epsilon}; g \rangle - \Gamma \frac{\gamma}{\Gamma} \sum_{\mathbf{k}', \epsilon'} \hbar \omega' \{ \dots \}^\dagger \cdot \left\{ \hbar^{-1} \int_0^t d\tau a_{\mathbf{k}', \epsilon'} \mathbb{U}_0(t - \tau) \right. \\
&\quad \left. \times e^{-\Gamma(t-\tau)/2} | (N-1)_{\mathbf{k}, \epsilon}; e \rangle \langle (N-1)_{\mathbf{k}, \epsilon}; e | \mathbf{d} \cdot \mathbf{E}(\mathbf{r}_A) | N_{\mathbf{k}, \epsilon}; g \rangle \langle N_{\mathbf{k}, \epsilon}; g | \mathbb{U}_0(\tau) | N_{\mathbf{k}, \epsilon}; g \rangle \right\} \\
&= \frac{\hbar \omega \gamma \Omega_0^2}{4} \left| \int_0^t d\tau e^{-i(t-\tau)\omega_0} e^{-(t-\tau)\Gamma/2} e^{-i\tau\omega} \right|^2,
\end{aligned} \tag{A5}$$

$$\begin{aligned}
\mathcal{W}^{(4)} &= \Gamma \left[\langle \Psi_4(0) | H_{EM} | \Psi_4(0) \rangle - \langle \Psi_4(t) | \Psi_4^f \rangle \langle \Psi_4^f | H_{EM} | \Psi_4^f \rangle \langle \Psi_4^f | \Psi_4(t) \rangle \right] \\
&= \Gamma \frac{\mathcal{P}}{\Gamma} \sum_{\mathbf{k}, \epsilon} \langle N_{\mathbf{k}, \epsilon}; e | \hbar \omega' a_{\mathbf{k}', \epsilon}^\dagger a_{\mathbf{k}', \epsilon} | N_{\mathbf{k}, \epsilon}; e \rangle - \Gamma \frac{\mathcal{P}}{\Gamma} \sum_{\mathbf{k}', \epsilon'} \hbar \omega' \{ \dots \}^\dagger \cdot \left\{ \hbar^{-1} \int_0^t d\tau a_{\mathbf{k}', \epsilon'} \mathbb{U}_0(t - \tau) \right. \\
&\quad \left. \times e^{-\Gamma(t-\tau)/2} | (N+1)_{\mathbf{k}, \epsilon}; g \rangle \langle (N+1)_{\mathbf{k}, \epsilon}; g | \mathbf{d} \cdot \mathbf{E}(\mathbf{r}_A) | N_{\mathbf{k}, \epsilon}; e \rangle \langle N_{\mathbf{k}, \epsilon}; e | \mathbb{U}_0(\tau) | N_{\mathbf{k}, \epsilon}; e \rangle \right\} \\
&= -\frac{\hbar \omega \mathcal{P} \Omega_0^2}{4} \left| \int_0^t d\tau e^{-2i(t-\tau)\omega} e^{-(t-\tau)\Gamma/2} e^{-i\tau(\omega + \omega_0)} \right|^2.
\end{aligned} \tag{A6}$$

Finally, the contributions of diagrams (5)–(7) of Fig. 3 to the incoherent power emitted spontaneously by the atom according to Eq. (19) are, respectively,

$$\begin{aligned}
\mathcal{W}^{(5)} &= \Gamma \left[\langle \Psi_5(t) | \Psi_5^f \rangle \langle \Psi_5^f | H_{EM} | \Psi_5^f \rangle \langle \Psi_5^f | \Psi_5(t) \rangle - \langle \Psi_5(0) | H_{EM} | \Psi_5(0) \rangle \right] \\
&= \Gamma \frac{\mathcal{P}}{\Gamma} \sum_{\mathbf{k}', \epsilon'} \hbar \omega' \{ \dots \}^\dagger \cdot \left\{ \hbar^{-1} \int_0^t d\tau a_{\mathbf{k}', \epsilon'} \mathbb{U}_0(t - \tau) e^{-\Gamma(t-\tau)/2} | 1_{\mathbf{k}', \epsilon'}, N_{\mathbf{k}, \epsilon}; g \rangle \langle 1_{\mathbf{k}', \epsilon'}, N_{\mathbf{k}, \epsilon}; g | \mathbf{d} \cdot \mathbf{E}_{\mathbf{k}', \epsilon'}^{(-)}(\mathbf{r}_A) | N_{\mathbf{k}, \epsilon}; e \rangle \right. \\
&\quad \left. \times \langle N_{\mathbf{k}_p, \epsilon_p}; e | \mathbb{U}_0(\tau) | N_{\mathbf{k}_p, \epsilon_p}; e \rangle \right\} \\
&= \mathcal{P} \int_0^\infty \frac{-dk' c^2 k'^3}{\epsilon_0 \pi} \boldsymbol{\mu} \cdot \text{Im} \mathbb{G}(\mathbf{R}; k') \cdot \boldsymbol{\mu} \left| \int_0^t d\tau e^{-i(t-\tau)\omega'} e^{-(t-\tau)\Gamma/2} e^{-i\tau\omega_0} \right|^2 \\
&\simeq -\mathcal{P} \int_0^\infty \frac{dk' c^2 k'^3 \boldsymbol{\mu} \cdot \text{Im} \mathbb{G}(\mathbf{R}; k') \cdot \boldsymbol{\mu}}{\epsilon_0 \pi (\omega' - \omega_0)^2 + \Gamma^2/4}, \quad \Gamma t \ll 1, R \rightarrow 0^+,
\end{aligned} \tag{A7}$$

$$\begin{aligned}
 \mathcal{W}^{(6)} + \mathcal{W}^{(7)} &= \Gamma \sum_{n=6}^7 [\langle \Psi_n(t) | \Psi_n^f \rangle \langle \Psi_n^f | H_{EM} | \Psi_n^f \rangle \langle \Psi_n^f | \Psi_n(t) \rangle - \langle \Psi_n(0) | H_{EM} | \Psi_n(0) \rangle] \\
 &= \Gamma \frac{-2\mathcal{P}}{\Gamma} \text{Re} \sum_{\mathbf{k}', \epsilon'} \hbar \omega' \hbar^{-4} \int_0^t d\xi \langle N_{\mathbf{k}, \epsilon}; e | \mathbb{U}_0^\dagger(\xi) | N_{\mathbf{k}, \epsilon}; e \rangle \langle N_{\mathbf{k}, \epsilon}; e | \mathbf{d} \\
 &\quad \cdot \mathbf{E}_{\mathbf{k}', \epsilon'}^{(+)}(\mathbf{r}_A) | 1_{\mathbf{k}', \epsilon'}, N_{\mathbf{k}, \epsilon}; g \rangle \langle 1_{\mathbf{k}', \epsilon'}, N_{\mathbf{k}, \epsilon}; g | a_{\mathbf{k}', \epsilon'}^\dagger \mathbb{U}_0^\dagger(t - \xi) e^{-\Gamma(t-\xi)/2} \\
 &\quad \times \int_0^t d\tau \int_0^\tau d\tau' \int_0^{\tau'} d\tau'' a_{\mathbf{k}', \epsilon'} \mathbb{U}_0(t - \tau) e^{-\Gamma(t-\tau)/2} | 1_{\mathbf{k}', \epsilon'}, N_{\mathbf{k}, \epsilon}; g \rangle \langle 1_{\mathbf{k}', \epsilon'}, N_{\mathbf{k}, \epsilon}; g | \mathbf{d} \cdot \mathbf{E}(\mathbf{r}_A) | 1_{\mathbf{k}', \epsilon'}, (N-1)_{\mathbf{k}, \epsilon}; e \rangle \\
 &\quad \times \langle 1_{\mathbf{k}', \epsilon'}, (N-1)_{\mathbf{k}, \epsilon}; e | \mathbb{U}_0(\tau - \tau') | 1_{\mathbf{k}', \epsilon'}, (N-1)_{\mathbf{k}, \epsilon}; e \rangle \langle 1_{\mathbf{k}', \epsilon'}, (N-1)_{\mathbf{k}, \epsilon}; e | \mathbf{d} \cdot \mathbf{E}(\mathbf{r}_A) | 1_{\mathbf{k}', \epsilon'}, N_{\mathbf{k}, \epsilon}; g \rangle \\
 &\quad \times \langle 1_{\mathbf{k}', \epsilon'}, N_{\mathbf{k}, \epsilon}; g | \mathbb{U}_0(\tau' - \tau'') e^{-\Gamma(\tau'-\tau'')/2} | 1_{\mathbf{k}', \epsilon'}, N_{\mathbf{k}, \epsilon}; g \rangle \langle 1_{\mathbf{k}', \epsilon'}, N_{\mathbf{k}, \epsilon}; g | \mathbf{d} \cdot \mathbf{E}_{\mathbf{k}', \epsilon'}^{(-)}(\mathbf{r}_A) | N_{\mathbf{k}, \epsilon}; e \rangle \langle N_{\mathbf{k}, \epsilon}; e | \mathbb{U}_0(\tau'') | N_{\mathbf{k}, \epsilon}; e \rangle \\
 &= \Omega_0^2 \mathcal{P} \text{Re} \int_0^\infty \frac{-dk' c^2 k'^3}{2\pi \epsilon_0} \boldsymbol{\mu} \cdot \text{ImG}(\mathbf{R}; k') \cdot \boldsymbol{\mu} \int_0^t d\tau e^{-i(t-\tau)(\omega'+\omega)} e^{-\Gamma(t-\tau)/2} \int_0^\tau d\tau' e^{-i(\tau-\tau')(\omega'+\omega_0)} e^{-(\tau-\tau')\Gamma/2} \\
 &\quad \times \int_0^{\tau'} d\tau'' e^{-i(\tau'-\tau'')(\omega'+\omega)} e^{-(\tau'-\tau'')\Gamma/2} e^{-i\tau''(\omega+\omega_0)} \int_0^{\tau''} d\xi e^{i(t-\xi)(\omega'+\omega)} e^{-\Gamma(t-\xi)/2} e^{i\xi(\omega+\omega_0)} \\
 &\simeq \frac{\Omega_0^2 \mathcal{P} c^2}{2\pi \epsilon_0} \text{Re} \int_0^\infty dk' k'^3 \boldsymbol{\mu} \cdot \text{ImG}(\mathbf{R}; k') \cdot \boldsymbol{\mu} \frac{e^{-it(\omega'-\omega)} - 1}{(\omega' - \omega)(\omega' - \omega_0 - i\Gamma/2)^2 (\omega' - \omega_0 + i\Gamma/2)}, \quad \Gamma t \gg 1, R \rightarrow 0^+.
 \end{aligned} \tag{A8}$$

- [1] J. J. Sakurai, *Advanced Quantum Mechanics* (Addison-Wesley, Boston, 1967).
- [2] P. W. Milonni, *The Quantum Vacuum* (Academic, San Diego, 1994).
- [3] M. E. Peskin and D. V. Schroeder, *An Introduction to Quantum Field Theory* (CRC/Taylor and Francis, New York, 2018).
- [4] B. A. van Tiggelen, in *Coherent Atomic Matter Waves*, edited by R. Kaiser, C. Westbrook, and F. David (Springer, Berlin, 2001), pp. 371–414.
- [5] P. R. Berman, R. W. Boyd, and P. W. Milonni, Polarizability and the optical theorem for a two-level atom with radiative broadening, *Phys. Rev. A* **74**, 053816 (2006).
- [6] P. W. Milonni, R. Loudon, P. R. Berman, and S. M. Barnett, Linear polarizabilities of two- and three-level atoms, *Phys. Rev. A* **77**, 043835 (2008).
- [7] S. Y. Buhmann, H. T. Dung, T. Kampf, and D. G. Welsch, Casimir-Polder interaction of atoms with magnetodielectric bodies, *Eur. Phys. J. D* **35**, 15 (2005).
- [8] P. de Vries, D. V. van Coevorden, and A. Lagendijk, Point scatterers for classical waves, *Rev. Mod. Phys.* **70**, 447 (1998).
- [9] L. S. Froufe-Pérez, R. Carminati, and J. J. Sáenz, Fluorescence decay rate statistics of a single molecule in a disordered cluster of nanoparticles, *Phys. Rev. A* **76**, 013835 (2007).
- [10] M. Donaire, Electromagnetic vacuum of complex media: Dipole emission versus light propagation, vacuum energy, and local field factors, *Phys. Rev. A* **83**, 022502 (2011); Electromagnetic vacuum of complex media. II. Lamb shift and total vacuum energy, **85**, 052518 (2012).
- [11] J. M. Wylie and J. E. Sipe, Quantum electrodynamics near an interface, *Phys. Rev. A* **30**, 1185 (1984).
- [12] L. Novotny and B. Hecht, *Principles of Nano-Optics* (Cambridge University Press, Cambridge, 2006).
- [13] F. Hynne and R. K. Bullough, The scattering of light I. The optical response of a finite molecular fluid, *Phil. Trans. R. Soc.* **A312**, 251 (1984); The scattering of light. II. The complex refractive index of a molecular fluid, **A321**, 305 (1987); The scattering of light III. External scattering from a finite molecular fluid, **A330**, 253 (1990).
- [14] R. K. Bullough, Many-body optics I. Dielectric constants and optical dispersion relations, *J. Phys.* **A1**, 409 (1968); Many-body optics II. Dielectric constant formulation of the binding energy of a molecular fluid, **A2**, 477 (1969); Many-body optics III. The optical extinction theorem and $\varepsilon(k, \omega)$, **A3**, 708 (1970); Many-body optics IV. The total transverse response and $\varepsilon_t(k, \omega)$, **A3**, 726 (1970); Many-body optics V. Virtual-mode theory, and phenomenological binding energies in the complex-dielectric-constant approximation, **A3**, 751 (1970).
- [15] G. S. Agarwal, Quantum electrodynamics in the presence of dielectrics and conductors. III. Relations among one-photon transition probabilities in stationary and nonstationary fields, density of states, the field-correlation functions, and surface-dependent response functions, *Phys. Rev. A* **11**, 253 (1975).
- [16] S. Y. Buhmann, H. Safari, D.-G. Welsch, and H. T. Dung, Microscopic Origin of Casimir-Polder Forces, *Open Syst. Inf. Dyn.* **13**, 427 (2006).
- [17] A. Lagendijk and B. van Tiggelen, Resonant multiple scattering of light, *Phys. Rep.* **270**, 143 (1996).
- [18] A. Salam, Intermolecular interactions in a radiation field via the method of induced moments, *Phys. Rev. A* **73**, 013406 (2006).
- [19] C. O'Brien, P. M. Anisimov, Y. Rostovtsev, and O. Kocharovskaya, Coherent control of refractive index in far-detuned Λ systems, *Phys. Rev. A* **84**, 063835 (2011).

- [20] C. Hang, G. Huang, and V. V. Konotop, \mathcal{PT} Symmetry with a System of Three-Level Atoms, *Phys. Rev. Lett.* **110**, 083604 (2013).
- [21] M. O. Scully and M. S. Zubairy, *Quantum Optics* (Cambridge University Press, Cambridge, 1997).
- [22] M. D. Lee, S. D. Jenkins, and J. Ruostekoski, Stochastic methods for light propagation and recurrent scattering in saturated and nonsaturated atomic ensembles, *Phys. Rev. A* **93**, 063803 (2016).
- [23] T. Binninger, V. N. Shatokhin, A. Buchleitner, and T. Wellens, Nonlinear quantum transport of light in a cold atomic cloud, *Phys. Rev. A* **100**, 033816 (2019).
- [24] W. Jin, C. Khandekar, A. Pick, A. G. Polimeridis, and A. W. Rodriguez, Amplified and directional spontaneous emission from arbitrary composite bodies: A self-consistent treatment of Purcell effect below threshold, *Phys. Rev. B* **93**, 125415 (2016).
- [25] A. Manjavacas, Anisotropic optical response of nanostructures with balanced gain and loss, *ACS Photon.* **3**, 1301 (2016).
- [26] E. del Valle, F. P. Laussy, and C. Tejedor, Luminescence spectra of quantum dots in microcavities. I. Bosons, *Phys. Rev. B* **79**, 235325 (2009); Luminescence spectra of quantum dots in microcavities. II. Fermions, **79**, 235326 (2009).
- [27] G. J. de Valcárcel, E. Roldán, and F. Prati, Semiclassical theory of amplification and lasing, *Rev. Mex. Fis. E* **52**, 198 (2006).
- [28] T. Savels, A. P. Mosk, and A. Lagendijk, Light scattering from three-level systems: The T matrix of a point dipole with gain, *Phys. Rev. A* **71**, 043814 (2005).
- [29] H. J. Carmichael, *Statistical Methods in Quantum Optics I* (Springer, Berlin, 1999).
- [30] H. Pau, *Introduction to Quantum Optics: From Light Quanta to Quantum Teleportation* (Cambridge University Press, Cambridge, 2004).
- [31] I. V. Hertel and C. P. Schulz, *Atoms, Molecules and Optical Physics 2* (Springer, New York, 2015).
- [32] C. Cohen-Tannoudji and S. Reynaud, Dressed-atom description of resonance fluorescence and absorption spectra of a multi-level atom in an intense laser beam, *J. Phys. B* **10**, 345 (1977).
- [33] C. M. Bender, \mathcal{PT} -symmetric quantum theory, *J. Phys.: Conf. Ser.* **631**, 012002 (2015).
- [34] Z. Zhang, Y. Zhang, J. Sheng, L. Yang, M.-A. Miri, D. N. Christodoulides, B. He, Y. Zhang, and M. Xiao, Observation of Parity-Time Symmetry in Optically Induced Atomic Lattices, *Phys. Rev. Lett.* **117**, 123601 (2016); Z. Zhang, D. Ma, J. Sheng, Y. Zhang, Y. Zhang, and M. Xiao, Non-hermitian optics in atomic systems, *J. Phys. B* **51**, 072001 (2018).
- [35] S. K. Özdemir, S. Rotter, F. Nori, and L. Yang, Parity-time symmetry and exceptional points in photonics, *Nat. Mater.* **18**, 783 (2019).
- [36] S. Sanders and A. Manjavacas, Nanoantennas with balanced gain and loss, *Nanophotonics* **9**, 473 (2020); M.-A. Miri, M. A. Eftekhar, M. Facao, A. F. Abouraddy, A. Bakry, M. A. N. Razvi, A. Alshahrie, A. Alú, and D. N. Christodoulides, Scattering properties of \mathcal{PT} -symmetric objects, *J. Opt.* **18**, 075104 (2016); A. Krasnok, D. Baranov, H. Li, M.-A. Miri, F. Monticone, and A. Alú, Anomalies in light scattering, *Adv. Opt. Photon.* **11**, 892 (2019); Y. J. Zhang, P. Li, V. Galdi, M. S. Tong, and A. Alú, Manipulating the scattering pattern with non-Hermitian particle arrays, *Opt. Express* **28**, 19492 (2020); R. Kolkowski and A. F. Koenderink, Gain-induced scattering anomalies of diffractive metasurfaces, *Nanophotonics* **9**, 4273 (2020).